

# Adaptive Sharpness-Aware Pruning for Robust Sparse Networks

Anna Bair  
CMU

abair@cmu.edu

Hongxu Yin  
NVIDIA

dannyy@nvidia.com

Maying Shen  
NVIDIA

mshen@nvidia.com

Pavlo Molchanov  
NVIDIA

pmolchanov@nvidia.com

Jose Alvarez  
NVIDIA

josea@nvidia.com

## Abstract

*Robustness and compactness are two essential components of deep learning models that are deployed in the real world. The seemingly conflicting aims of (i) generalization across domains as in robustness, and (ii) specificity to one domain as in compression, are why the overall design goal of achieving robust compact models, despite being highly important, is still a challenging open problem. We introduce Adaptive Sharpness-Aware Pruning, or AdaSAP, a method that yields robust sparse networks. The central tenet of our approach is to optimize the loss landscape so that the model is primed for pruning via adaptive weight perturbation, and is also consistently regularized toward flatter regions for improved robustness. This unifies both goals through the lens of network sharpness. AdaSAP achieves strong performance in a comprehensive set of experiments. For classification on ImageNet and object detection on Pascal VOC datasets, AdaSAP improves the robust accuracy of pruned models by +6% on ImageNet C, +4% on ImageNet V2, and +4% on corrupted VOC datasets, over a wide range of compression ratios, saliency criteria, and network architectures, outperforming recent pruning art by large margins.*

## 1. Introduction

Deep neural networks have increasingly been used in many applications such as autonomous driving. Unlike the controlled environments in which these models are trained, test-time inference presents new challenges including noisy real-world data, and latency and memory constraints. These challenges have led to recent efforts in network robustness and compression, but through largely separate lines of work.

Robustness to input variation is especially important for deployed deep learning models in safety-critical applications such as autonomous driving, where artifacts such as dirt or snow may obscure the camera image. More gener-

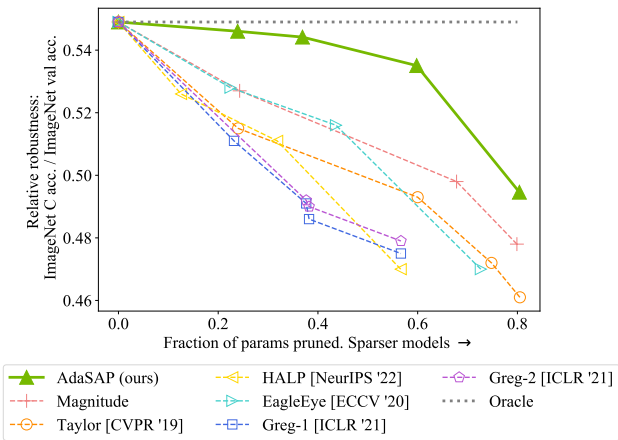


Figure 1: Robustness of pruned models on ImageNet-1K drastically degrades on ImageNet-C as pruning ratio increases for many SOTA pruning methods. Our AdaSAP method reduces the degradation in robust performance relative to standard validation performance. We approach the grey dashed line, which indicates an ideal scenario in which robust performance does not degrade at higher rates than the standard validation performance.

ally, in computer vision (CV) applications, this input variation falls into categories including distribution shifts, image corruptions, adversarial attacks, and label noise [24, 2, 6, 7, 25, 55]. In attempts to address these challenges, the vision community has collected and released datasets to assess model robustness [24, 50] and multiple lines of work have both investigated and improved performance on a variety of types of robustness [64, 71, 57, 45]. Despite significant progress in this area, much of the existing robustness work focuses on dense networks.

Running large, dense models imposes substantial computational burdens that can be addressed via model compression methods. The main insight of this line of work

is to reduce network inference costs via techniques such as knowledge distillation [26, 46, 67], quantization [19, 3, 32, 5], pruning [21, 65, 69, 48, 47, 53], and network adaptation [46, 9, 66], leveraging the observation that neural networks often include redundant computation at inference. Among these techniques, pruning is widely adopted due to its simple process of network speedup, so we choose to focus on pruning in this work. Since the pruning process removes parameters deemed insignificant over the target distribution, resulting networks can have reduced out-of-distribution (OOD) generalization performance as observed in previous work [41, 29] and verified in our experiments. The effort to jointly address robustness and compression challenges remains an open problem.

The primary goal of our work is to produce compact and robust neural networks. At first glance, it might seem as if the goals of sparsity and robustness are at odds – one aims to exploit the current dataset and task for extreme compactness whereas the other strives for maximal generalization. However, a closer look into their objective functions proves otherwise. More specifically, we leverage a new flatness-based optimization procedure that both primes the network for optimal pruning and also improves network robustness.

We introduce *Adaptive Sharpness-Aware Pruning* (*AdaSAP*), a three-step fine-tuning algorithm that prunes a pre-trained network so that it is robust to corrupted inputs. (1) We first introduce *adaptive weight perturbations* as part of the optimization procedure to prepare the network for pruning. This step enforces that neurons which are likely to be pruned are situated in flatter minima, thus minimally impacting the loss once they are pruned. (2) We then apply any structured pruning method to the model, and (3) continue training the model to convergence while uniformly penalizing sharpness across the network in order to encourage robustness.

*AdaSAP* significantly improves the robustness performance over prior pruning art, as shown in Figure 1. As models are pruned more, the degradation of their performance on corrupted images suffers disproportionately as compared to their validation performance, which highlights the lack of robustness preservation in recent SOTA pruning methods and *AdaSAP*’s success at reducing this degradation<sup>1</sup>.

Our contributions can be summarized as follows:

- We introduce *AdaSAP*, a sharpness-aware pruning and fine-tuning process to jointly optimize for sparsity and robustness in deep neural networks.
- We propose *adaptive weight perturbations* that prepare a network for both pruning and robustness to OOD in-

<sup>1</sup>Relative robustness in Fig. 1 refers to the ratio between the accuracy on corrupted images and the standard validation accuracy at a given prune ratio. A dense model in this setup retains 55% of its validation performance when given corrupted images (location of grey dashed line).

puts. This strategy actively manipulates the flatness of the loss surface so as to minimize the impact of removing neurons with lower importance scores.

- We demonstrate state-of-the-art performance compared to prior art by noticeable margins across a wide range of setups, covering (i) two tasks (classification and detection), (ii) two OOD types (image corruption and distribution shift), (iii) four networks (ResNet50 and MobileNet V1/V2 for classification, SSD512 for detection), (iv) two pruning paradigms (parameter-based and latency-based), and (v) a wide range of sparsity ratios spanning from 25% to 80%.
- We present a detailed evaluation of robustness and compactness and show, as a first encouraging attempt, that both goals can be unified through the lens of sharpness, with analysis to encourage the community to continue pursuing this direction.

## 2. Related Works

**Robustness.** Researchers and practitioners care about many types of robustness, including adversarial robustness, robustness to distribution shift, robustness to image corruptions such as weather effects, and robustness to label noise or data poisoning [57, 45, 24, 2, 6, 7, 25, 55]. Several prior works examine the adversarial robustness of sparse networks [52, 18]. Simultaneously, work such as [56] suggests that adversarially robust networks have flatter minima.

In this work we primarily focus on robustness to corrupted images [24, 50] due to its application in settings such as autonomous driving. Prior work has analyzed the robustness of pruned models. [12] shows that sparse subnetworks can outperform the dense model on clean and robust accuracy. However, almost all current pruning methods still lead to worse performance on OOD data than dense networks, a result we replicate in Figure 1 [41, 29].

**Efficiency.** Efforts to improve network efficiency include pruning, distillation, quantization, and adaptation [21, 65, 69, 48, 47, 53, 26, 19, 3, 46, 9, 66]. We focus on pruning as a model compression method. The two broad categories of pruning include structured and unstructured pruning. While unstructured pruning removes individual weights and can retain strong performance at higher sparsities, structured pruning removes entire structures in the network, such as convolutional channels, and often allows for direct latency reduction of the pruned model. Unstructured pruning dates back to the optimal brain damage paper, but the Lottery Ticket Hypothesis has incited recent interest in the topic and spurred other developments such as SNIP and GraSP [39, 17, 28, 38, 58, 59, 70]. In the current work, we focus on structured channel-wise pruning due to the easily obtained speedups. [1] outlines various structured pruning methods. By pruning larger structural elements within a

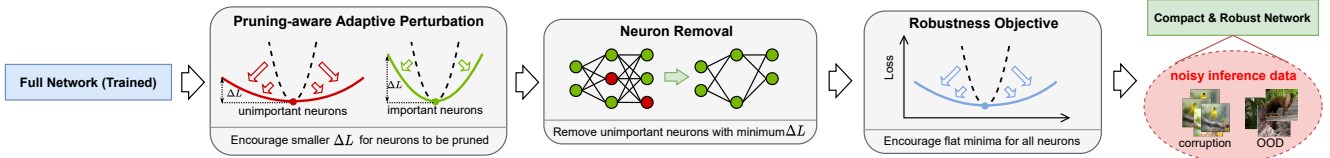


Figure 2: AdaSAP is a three step process that takes as input a dense pretrained model and outputs a sparse robust model. The process can be used with any pruning method.

network, such as kernels or filters, rather than simply individual weights, the pruned elements can be removed and more directly lead to speed gains [47, 53].

**Flat Minima.** The relationship between flat minima and generalization has been studied for many years [27, 36, 63, 20, 34, 62, 4, 8, 33, 35]. Flat minima are generally correlated with improved generalization performance, but the investigations into the extent of this correlation and the underlying causal relationship are still ongoing. It is also important to note that flatness is metric-dependent and it is possible for sharp minima to generalize well [13]. Sharpness-Aware Minimization (SAM) [16] is a way to optimize for finding flatter minima and leads to better generalization. Some work builds upon SAM, including improving the efficiency of the method [43, 14], modifying the optimization for improved performance [37] and applying it for improved model compression in NLP tasks [49]. Stochastic weight averaging (SWA) is another method that has been used to optimize for flatter minima [33, 8] and has been compared to SAM [35]. The present work is inspired by SAM and its use in model compression [16, 49] but differs in its use of adaptive weight perturbations and its emphasis on the robustness of pruned models. In this work we use the formulation introduced in ASAM [37] due to its improved performance over that of SAM.

### 3. The AdaSAP Method

The main objective of our design is to find minima within relatively large regions of the parameter space that have low loss (*i.e.*, flat minima), in order to produce models that are simultaneously prunable and robust. Previous work has shown that flatter minima improve generalization [16] and adversarial robustness [56] in dense networks and generalization in sparse networks [49]. We hypothesize that optimizing for flatter minima during the pruning process can also enhance robustness.

We introduce a new method, Adaptive Sharpness-Aware Pruning (AdaSAP). Figure 2 and Algorithm 2 detail the method’s three step procedure, which we describe below:

**Adaptive Weight Perturbation.** We first warm up the model for pruning. During this process we ensure that the neurons that will be pruned, are regularized to lie in flat regions so that they will not cause the model’s performance to suffer too much after pruning.

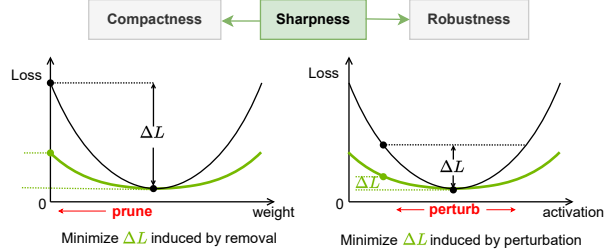


Figure 3: Before pruning (left), we want to encourage neurons that will be pruned to lie within a flat minima, since their removal will affect the loss less. After pruning (right), we promote robustness by uniformly encouraging flatness across the network.

**Neuron/Channel Removal.** We conduct structured channel-wise pruning and remove neurons according to any existing pruning criteria, such as magnitude or Taylor importance [48]. The model is easily prunable since unimportant neurons have been situated in flatter loss regions.

**Robustness Encouragement.** While training the pruned model to convergence, we again enforce flat minima, this time uniformly (*i.e.*, non-adaptively) across the entire network to promote robustness. This step is compatible with any flatness-based optimizer. In this work, we use SAM [16] and ASAM [37].

#### 3.1. Adaptive Weight Perturbation

Our procedure performs gradient updates which are informed by the local flatness in order to best prepare the network for pruning. We adapt the robustness regularization per neuron based on the likelihood of that neuron to be pruned. Pruning can be viewed as a special case of directional robustness, in which the weight and activation of a pruned neuron are set to zero. When the loss landscape is flat, the pruning process will incur only a small impact on the performance of the model. This formulation indicates that pruning and robustness share a common objective through the perspective of sharpness, as demonstrated in Figure 3.

Taking inspiration from the uniform  $\epsilon$ -ball perturbation based method in [16] and its scale-invariant version in [37], among several other approaches to flatness in dense models [33, 51], we perturb neurons according to their import-

tance to better prepare the network for pruning. We adapt the size of allowable perturbations based on the likelihood of each weight to be pruned: weights with a small score have a large perturbation ball which enforces that it lies within a flatter region, while weights with a large score have a small perturbation ball. This rationale that important weights are worth adding some sharpness to the model is corroborated by work which shows that pruning neurons in flat regions hurts the loss less than pruning neurons in sharp regions [47].

Following this intuition, we now derive the gradient update for training using our AdaSAP method. Consider a network with  $I$  neurons in total, where each neuron indexed as  $i$  has associated weights  $w_i$ .

For instance, if each network parameter belongs to its own partition, we have unstructured pruning. In our setting, each channel belongs to its own partition. Throughout this paper we refer to a channel-wise group of weights as a *neuron*. We use  $w_i$  to refer to a single neuron and  $\mathbf{w}$  to refer to the collection of all neurons  $\{w_i\}$ .

Consider training loss  $L_S(\mathbf{w})$  of the network over the training dataset  $S$ . In order to quantify our weight perturbation, we consider a set of perturbation ball radius sizes  $\rho$ , with each  $\rho_i$  corresponding to the size of allowable perturbations for neuron  $w_i$ . Given this notation, the goal of our warmup procedure is to optimize for a network with a flatter minimum for unimportant neurons prior to pruning via the following objective

$$\min_{\mathbf{w}} \max_{\{\|T_{\mathbf{w}}^{-1}\epsilon_i\|_2 \leq \rho_i\}_{i=1}^I} L_S(\mathbf{w} + \epsilon). \quad (1)$$

where  $T_{\mathbf{w}}$  and its inverse  $T_{\mathbf{w}}^{-1}$  are transformations that can be applied during optimization so as to reshape the perturbation region (*i.e.*, not necessarily a ball). This strategy was studied in [37] in order to allow for greater perturbation exploration and leads to improved performance.

We determine the values  $\rho_i$  based on computing an importance score for each neuron, similar to a pruning criterion. Consider a neuron importance score function  $\psi(\cdot)$ , such as the  $\ell_2$  norm of the neuron weight, the Taylor importance score [48], or other scores that are often some function of weights, gradients, and higher order terms [39, 70, 53, 59]. Given the scores for each neuron as  $s_i = \psi(w_i)$ , we can now compute a re-weighting factor  $\alpha_i$  that maps the range of scores to the desired range of perturbation sizes

$$\alpha_i = s_{\max} - \frac{s_i - s_{\min}}{s_{\max} - s_{\min}} (\rho_{\max} - \rho_{\min}), \quad (2)$$

which leads to the perturbation ball size  $\rho_i$  of a neuron  $i$ :

$$\rho_i = -\alpha_i s_i. \quad (3)$$

Scores  $s_{\min}$  and  $s_{\max}$  are obtained empirically at each gradient step, but  $\rho_{\max}$  and  $\rho_{\min}$  are global algorithm hyperparameters that are set ahead of time and we find them to scale across various experiment settings (further details in Section 4). Note that due to the progress in pruning literature, neuron importance estimates  $\psi(\cdot)$  can be evaluated during training with little additional computational overhead.

Our enhanced gradient update optimizes for finding a minimum that also lies in a region of low loss. Beginning with our objective in Eq. 1, we perform a series of approximations in order to find the most adversarial perturbations  $\epsilon = \{\epsilon_i\}$  which we can apply correspondingly to the neurons  $\mathbf{w} = \{w_i\}$  in our network in order to obtain a flatness-informed gradient update.

We use a first order Taylor expansion around each neuron  $i$  with respect to  $\epsilon$  around 0 (in line with [16]) to approximate the inner maximization in Eq. 1. This gives us  $\epsilon^*$ , the optimal  $\epsilon$  we can use to inform our gradient update. Define  $\tilde{\epsilon}_i = T_{\mathbf{w}}^{-1}\epsilon_i$ . For simplicity we denote the conditional loss due to weight perturbations as the function  $L_{S,\mathbf{w}}(\cdot)$ . Then we derive our optimal update as follows for each neuron:

$$\begin{aligned} \tilde{\epsilon}_i^* &= \arg \max_{\|\epsilon_i\|_2 \leq \rho_i} L_{S,\mathbf{w}}(w_i + T_{\mathbf{w}}\tilde{\epsilon}_i), \\ &\approx \arg \max_{\|\tilde{\epsilon}_i\|_2 \leq \rho_i} L_{S,\mathbf{w}}(w_i) + \tilde{\epsilon}_i^\top T_{\mathbf{w}} \nabla_{w_i} L_{S,\mathbf{w}}(w_i), \\ &= \arg \max_{\|\tilde{\epsilon}_i\|_2 \leq \rho_i} \tilde{\epsilon}_i^\top T_{\mathbf{w}} \nabla_{w_i} L_{S,\mathbf{w}}(w_i), \end{aligned} \quad (4)$$

$\|\cdot\|_2$  being the  $\ell_2$  norm. We can then approximate  $\tilde{\epsilon}^*$  by rescaling the gradient associated with each neuron so that its norm is  $\rho_i$  through

$$\tilde{\epsilon}_i^* = \rho_i \frac{\text{sign}(\nabla_{w_i} L_{S,\mathbf{w}}(w_i)) |T_{\mathbf{w}} \nabla_{w_i} L_{S,\mathbf{w}}(w_i)|}{(\|T_{\mathbf{w}} \nabla_{w_i} L_{S,\mathbf{w}}(w_i)\|_2^2)^{1/2}}. \quad (5)$$

Since we were originally approximating  $\tilde{\epsilon}_i = T_{\mathbf{w}}^{-1}\epsilon_i$ , we recover our approximation of  $\epsilon^*$  as

$$\hat{\epsilon}_i = \rho_i \frac{T_{\mathbf{w}}^2 \nabla_{w_i} L_{S,\mathbf{w}}(w_i)}{\|\nabla_{w_i} L_{S,\mathbf{w}}(w_i)\|_2}. \quad (6)$$

We then find an approximation to our desired gradient. Referring to Eq. 1, we can find the gradient of the inner maximization in order to derive a sharpness-aware gradient update. We use the inner maximization and plug in our approximation  $\hat{\epsilon}$  for each individual neuron during adjacent pruning steps, defined as

$$\begin{aligned} \nabla_{w_i} \max_{\|T_{\mathbf{w}}^{-1}\epsilon_i\|_2 \leq \rho_i} L_{S,\mathbf{w}}(w_i + \epsilon_i) &\approx \nabla_{w_i} L_{S,\mathbf{w}}(w_i + \hat{\epsilon}_i) \\ &= \frac{d(w_i + \hat{\epsilon}_i)}{dw_i} \nabla_{w_i} L_{S,\mathbf{w}}(w_i)|_{w_i + \hat{\epsilon}_i} \\ &= \nabla_{w_i} L_{S,\mathbf{w}}(w_i)|_{w_i + \hat{\epsilon}_i} \\ &\quad + \frac{d\hat{\epsilon}_i}{dw_i} \nabla_{w_i} L_{S,\mathbf{w}}(w_i)|_{w_i + \hat{\epsilon}_i} \\ &\approx \nabla_{w_i} L_{S,\mathbf{w}}(w_i)|_{w_i + \hat{\epsilon}_i}, \end{aligned} \quad (7)$$

---

**Algorithm 1** AdaSAP Optimization Iteration

---

**Input:** model weights  $\mathbf{w}$  partitioned into neurons  $w_i$ , training batch  $b$ ,  $\rho$  bounds  $(\rho_{\min}, \rho_{\max})$ , loss  $L$ , score function  $\psi$ , learning rate  $\eta$

```

for each neuron  $w_i$  do
     $s_i = \psi(w_i)$                                  $\triangleright$  Score
    Compute  $\alpha_i$  as in Eq. 2                     $\triangleright$  Rescaling scores
     $\rho_i = -\alpha_i s_i$                           $\triangleright$  Determine perturbation ball size
    Compute  $\hat{\epsilon}_i$  as in Eq. 6                 $\triangleright$  Optimal perturbation
     $g_i \approx \nabla_{w_i} L_{b, \mathbf{w}}(w_i)|_{w_i + \hat{\epsilon}_i}$   $\triangleright$  Gradient approximation
end for
 $\mathbf{w} = \mathbf{w} - \eta \mathbf{g}$ 
return  $\mathbf{w}$ 

```

---

where we drop the second order terms for efficiency. This leads us to our final gradient update approximation between adjacent pruning steps as

$$\nabla_{w_i} L_{S, \mathbf{w}}(w_i) \approx \nabla_{w_i} L_{S, \mathbf{w}}(w_i)|_{w_i + \hat{\epsilon}_i}. \quad (8)$$

We use this gradient update in the place of the standard gradient update during the warmup phase of our pruning procedure before each neuron removal step. This sets up our network so that when pruning begins, we have a model that is closer to a flat minima. The details of the optimization procedure are in Algorithm 1.

### 3.2. Neuron Removal

We focus on structured pruning since it leads to models that can take advantage of direct computational resource savings on GPUs, leading to inference speedup [46, 53, 65]. While unstructured pruning can often lead to more performant models at higher levels of pruning, it is not as easy to produce smaller models with latency speedups, and so due to the desire for practical applicability of our method, we limit our analysis here to structured pruning.

In this stage of the procedure, we remove unimportant neurons according to some scoring function  $\phi(\cdot)$  as in any pruning method that uses a measure of neuron saliency. Note that this may be the same or different from the scoring function  $\psi(\cdot)$  used in determining adaptive weight perturbation ball sizes during the first step. AdaSAP works with a range of pruning methods as we show later in Section 4.

### 3.3. Robustness Encouragement

In the third and final phase, we focus on optimizing our model for robust performance. Again, we seek to move our weights toward flat minima, but this time we want to regularize them all uniformly because our main goal is to ensure that all weights are in relatively flat minima since this will encourage robust performance. This is illustrated in Figure 3 in the plot on the right: the network loss relative to a flatter neuron will stay more stable in the presence of corruptions, whereas the loss relative to a sharper neuron could fluctuate significantly. This portion of the procedure could be instantiated with any sharpness-based method that optimizes for

---

**Algorithm 2** AdaSAP Pruning Procedure

---

**Input:** Pretrained model weights  $\mathbf{w}$  partitioned into neurons  $w_i$ , pruning importance criteria  $\phi$ ,  $\rho$  bounds  $(\rho_{\min}, \rho_{\max})$

```

Let  $\text{train\_iter}$  = Algorithm 1
for epoch in warmup_epochs do                                 $\triangleright$  Adaptive Weight Perturbation
    for each iteration do
        Sample training batch  $b$ 
         $\mathbf{w} = \text{train\_iter}(\mathbf{w}, b, \rho_{\min}, \rho_{\max})$ 
    end for
end for
for epoch in pruning_epochs do                                 $\triangleright$  Pruning
    for each iteration do
        Sample training batch  $b$ 
         $\mathbf{w} = \text{train\_iter}(\mathbf{w}, b, \rho_{\min}, \rho_{\max})$ 
        if iteration % prune_frequency = 0 then
             $s = \phi(\mathbf{w})$                                  $\triangleright$  Score all neurons
             $\text{idxs} = \text{rank}(s)[: \text{prune\_num}]$            $\triangleright$  Neurons with lowest score
             $\mathbf{w}_{\text{idxs}} = 0$                                  $\triangleright$  Prune neurons
        end if
    end for
end for
for epoch in finetune_epochs do                                 $\triangleright$  Robustness encouragement
    for each iteration do
        Sample training batch  $b$ 
         $\mathbf{w} = \text{train\_iter}(\mathbf{w}, b, \rho_{\min} = \rho_{\max} = \text{constant})$        $\triangleright$  SAM
    end for
end for
return  $\mathbf{w}$ 

```

**Output:** Pruned and finetuned model

---

an overall flatter minima, given that the network is already compressed.

### 3.4. Final Paradigm

We emphasize that AdaSAP *is not a pruning method* but rather an optimization paradigm that performs robustness-aware pruning. Our method can be used in conjunction with any existing pruning criteria. In Section 4 we show that AdaSAP generally outperforms existing SOTA pruning methods. As new pruning techniques arise, they could be enhanced via AdaSAP in order to obtain increased performance, particularly robustness performance.

## 4. Experiments & Results

We next examine the performance of AdaSAP. In this section, we first discuss our experimental setup, and then demonstrate the effectiveness of our approach on several datasets compared to other SOTA methods. Finally, we discuss and analyze different aspects of our method and evaluate variations of the algorithm.

### 4.1. Experiment Details

**Datasets.** We use the ImageNet-1K dataset [11] for our image classification experiments. To evaluate the robustness and generalization ability of the pruned models, we additionally evaluate models on the ImageNet-C [24] and ImageNet-V2 [50] datasets. For object detection, we use the Pascal VOC dataset [15]. In order to assess robustness to corruptions, we create a Pascal VOC-C dataset by applying ImageNet-C-style corruptions to the test set.

**Network Architectures.** In our experiments we prune three different networks for the classification task: ResNet50, MobileNetv1 and MobileNetv2 [22, 30]. We use a pre-trained model trained for 90 epochs with a cosine learning rate as in HALP [54] and EagleEye [40]. For object detection, we follow the experimental setup in HALP [54] to prune an SSD512 model with ResNet50 as the backbone. We perform Distributed Data Parallel training across 8 V100 GPUs with batch size 128 for all experiments.

**Pruning Schedule.** Given a pre-trained model, for any architecture, we run the warm up for 10 epochs, and then we follow the same pruning schedule as in [10]: we prune every 30 iterations and, in each iteration, we prune away a  $p_r$  fraction of neurons so that the final network is pruned by a fraction  $p$  (resulting in a network of size  $1 - p$ ). To determine the  $p_r$  fraction, we follow an exponential decay schedule. Let  $k = 1 - p$  and let  $k_r$  be the number of neurons remaining after  $r$  pruning iterations, where the total number of pruning iterations is  $R$ . Let  $m$  be the number of neurons in the dense network, and define  $\alpha = \frac{r}{R}$ . Then,  $k_r = \exp\{\alpha \log k + (1 - \alpha \log m)\}$ . We fine-tune the pruned model for another 79 epochs (to reach 90 epochs total).

**Pruning Criteria.** Our proposal is agnostic to the particular importance criteria  $\phi$  used to prune the network. We evaluate our method on two types of pruning: *parameter-based* and *latency-based*. We choose to group our methods into these two categories due to the different goals of pruning methods. In general, pruning is beneficial because it produces smaller and faster models. Some methods, such as Taylor [47] and magnitude pruning, seek to reduce the number of parameters to produce a small model. Other methods, such as HALP [54], seek to produce a model with the fastest latency speedup, regardless of the number of parameters.

In both cases, we perform structured pruning, that is, pruning channels rather than individual parameters. We refer to our two methods as AdaSAP<sub>P</sub> and AdaSAP<sub>L</sub>, to denote the parameter-specific method and the latency-specific method, respectively. We use  $\ell_2$  norm magnitude pruning for AdaSAP<sub>P</sub> and HALP for AdaSAP<sub>L</sub>.

**Metrics.** For image classification, we report the top1 accuracy of the pruned models on the ImageNet validation set, the ImageNet C dataset, and the ImageNet V2 dataset. Additionally, we report two *robustness ratios*:  $R_C$  and  $R_{V2}$ , defined as the ratio in top1 accuracy on the robustness dataset to the top1 accuracy on the validation set. That is,  $R_C = \text{acc}_C / \text{acc}_{val}$  and  $R_{V2} = \text{acc}_{V2} / \text{acc}_{val}$ . We use these metrics to measure the robust performance relative to standard validation performance. An improvement in these robustness ratios indicates that we are closing the gap between robust and validation performance.

For object detection, we evaluate the model on the Pascal VOC test set as well as our VOC-C dataset with corrupted images. We report mean average precision (mAP) and a

similar robustness ratio  $R_C = \text{mAP}_C / \text{mAP}_{val}$ .

**Hyperparameters.** We use ASAM <sup>2</sup> [37], a recent improvement upon SAM, in our implementation of AdaSAP. The base optimizer is SGD with cosine annealing learning rate with a linear warmup over 8 epochs, a largest learning rate of 1.024, momentum at 0.875, and weight decay  $3.05e - 05$ . Unless otherwise stated we use  $\rho_{min} = 0.01$  and  $\rho_{max} = 2.0$  for all experiments – we observe these values scale well across networks and tasks. For robustness encouragement we use  $\rho = 2.0$  in line with prior work [37]. For some ablation experiments, the original SAM [16] optimizer is sufficient and in these cases we reduce  $\rho_{max} = 0.1$  and use constant  $\rho = 0.05$  for finetuning, with exact usage specified in the corresponding experiment and ablation sections.

**Baselines.** We primarily focus on comparing to two SOTA baselines, Taylor pruning for parameter-based pruning [47], and HALP [53] for latency-based pruning. Taylor pruning assigns a score to each neuron based on a Taylor series approximation of how much the loss would change if the neuron were removed [48, 47]. On the other hand, HALP is a pruning method that optimizes for improving latency [54]. In addition to these methods, we compare to several other pruning methods such as GR-eg [60] and EagleEye [40] as well as magnitude pruning, which is a strong baseline.

## 4.2. ImageNet Classification

**Parameter Reduction.** We instantiate our AdaSAP<sub>P</sub> method with a magnitude importance score ( $\phi = \|\cdot\|_2$ ). We compare our results to other pruning methods in the literature. The summaries of results for different pruning ratios are shown in Table 1 for ResNet50. MobileNet (V1 and V2) results show a similar trend and are included in the appendix. Our method compares favorably in several ways. First, AdaSAP has the best overall  $R_C$  and  $R_{V2}$  ratios among all pruning methods. This means that our method helps to close the gap between robust performance and standard validation performance. Additionally, our method consistently outperforms comparisons on both ImageNet validation performance and on robust performance (via ImageNet C and ImageNet V2) while at the same or even smaller compressed model size. Note that the only instance of our model not achieving the best performance across any metric is when it is compared with a model that has 4% more parameters (and it still only underperforms on ImageNet V2 and  $R_{V2}$ ).

**Latency Reduction.** In a second set of experiments, we instantiate our algorithm to focus on latency constraints. To this end, we consider the most recent hardware-aware pruning method HALP (NeurIPS’23 [54]), which incorporates

<sup>2</sup>ASAM [37] applies a scale-invariant transformation so that the perturbation region can vary in shape (*i.e.* not limited to a ball).

Method - % Pruned	Size ↓	Val	$R_{V2}$	$R_C$	IN-V2	IN-C
<b>ResNet50</b>						
Dense	1	77.32	0.83	0.55	64.79	42.46
Magnitude - 80%	0.20	73.80	0.83	0.48	61.40	35.27
Taylor - 80% [47]	0.20	73.56	0.82	0.46	60.56	33.93
EagleEye 1G - 73% [40]	0.27	74.13	0.83	0.47	61.30	34.84
<b>AdaSAP<sub>P</sub> - 80% (Ours)</b>	<b>0.20</b>	<b>74.63</b>	<b>0.83</b>	<b>0.50</b>	<b>62.08</b>	<b>37.30</b>
Magnitude - 56%	0.44	76.83	<b>0.85</b>	0.51	<b>64.92</b>	39.27
Taylor - 58% [47]	0.42	75.85	0.84	0.50	63.51	37.84
Greg-1 - 57% [61]	0.43	73.72	0.82	0.48	60.47	35.04
Greg-2 - 57% [61]	0.43	73.84	0.83	0.48	61.05	35.39
ABCPruner - 56% [42]	0.44	73.52	0.82	0.50	60.46	36.64
<b>AdaSAP<sub>P</sub> - 58% (Ours)</b>	<b>0.40</b>	<b>77.27</b>	0.83	<b>0.53</b>	64.51	<b>41.23</b>
Greg-1 - 38% [61]	0.62	75.16	0.82	0.49	61.82	36.88
Greg-2 - 38% [61]	0.62	75.36	0.82	0.49	62.06	37.09
ABCPruner - 29% [42]	0.71	74.84	0.83	0.51	61.73	38.35
<b>AdaSAP<sub>P</sub> - 38% (Ours)</b>	<b>0.62</b>	<b>77.99</b>	<b>0.84</b>	<b>0.52</b>	<b>65.49</b>	<b>42.68</b>
Magnitude - 24%	0.76	77.32	0.84	0.53	65.20	40.73
Taylor - 24% [47]	0.76	77.05	0.84	0.52	64.53	39.68
Greg-1 - 23% [61]	0.77	76.25	0.83	0.51	63.61	38.96
EagleEye 3G - 22% [40]	0.78	77.07	0.84	0.53	64.84	40.67
<b>AdaSAP<sub>P</sub> - 23% (Ours)</b>	0.77	<b>78.29</b>	<b>0.84</b>	<b>0.55</b>	<b>66.14</b>	<b>43.22</b>

Table 1: **ResNet50 - Parameter Reduction.** Top1 Accuracy as a function of the pruning ratio.

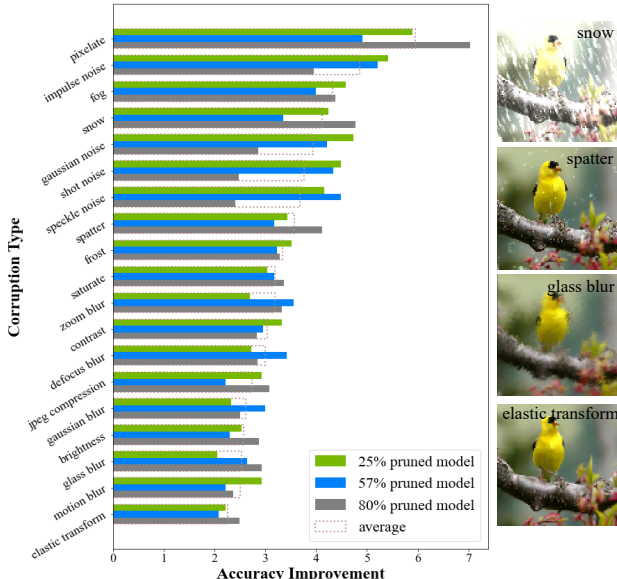


Figure 4: Performance difference on various ImageNet C corruption types on models of varying sparsity. Accuracy improvement is the Top1 accuracy on a model trained with AdaSAP minus that of a Taylor pruned model.

latency into the metric to measure the saliency of each neuron in the network.

Similarly to the parameter-based pruning method, Table 2 shows that using AdaSAP in conjunction with HALP outperforms prior works both in terms of the  $R_C$  and  $R_{V2}$  ratios, and also in terms of standard validation performance and performance on robust datasets.

Method - % Pruned	Speedup ↑	Size ↓	Val	$R_{V2}$	$R_C$	IN-V2	IN-C
<b>ResNet50</b>							
Dense	1	77.32	0.83	0.55	64.79	42.46	
HALP - 70% [54]	2.6	0.43	74.46	0.82	0.47	61.21	35.03
<b>AdaSAP<sub>L</sub> - 70% (Ours)</b>	2.6	0.41	<b>75.37</b>	<b>0.83</b>	<b>0.50</b>	<b>62.61</b>	<b>37.93</b>
HALP - 45% [54]	1.6	0.68	76.55	0.83	0.51	63.62	39.13
SMCP - 50% [31]	1.7	0.60	76.62	0.83	0.51	63.86	38.72
<b>AdaSAP<sub>L</sub> - 45% (Ours)</b>	1.6	0.65	<b>77.28</b>	<b>0.85</b>	<b>0.54</b>	<b>65.35</b>	<b>41.63</b>
HALP - 20% [54]	1.2	0.87	77.45	0.84	0.53	64.88	40.77
SMCP - 20% [31]	1.2	0.87	77.57	0.84	0.53	65.02	40.91
<b>AdaSAP<sub>L</sub> - 20% (Ours)</b>	1.1	0.82	<b>77.93</b>	0.84	<b>0.55</b>	<b>65.53</b>	<b>42.92</b>

Table 2: **ResNet50 - Latency Reduction.** Top1 accuracy for latency constrained pruning for various speedup ratios.

Method - % Pruned	Val	Corrupted	$R_C$
HALP - 60% [53]	0.774	0.583	0.753
<b>AdaSAP - 60% (Ours)</b>	<b>0.795</b>	<b>0.620</b>	<b>0.780</b>
HALP - 80% [53]	0.770	0.580	0.753
<b>AdaSAP - 80% (Ours)</b>	<b>0.793</b>	<b>0.616</b>	<b>0.776</b>

Table 3: **Object Detection.** mAP on validation images and ImageNetC style corruptions on the Pascal VOC dataset.

### 4.3. Object Detection

We show the object detection pruning results in Table 3. We run experiments for 800 epochs, where the first 50 epochs encompass the pruning stage (and where adaptive weight perturbations are applied). After pruning has completed, we switch to uniform perturbations. We choose the checkpoint within the last 30 epochs that has the highest mAP on validation and use that checkpoint to evaluate on corrupted images, where the averaged mAP over 18 different corruption types is reported. These results do not use ASAM-augmented AdaSAP. Across two pruning levels, AdaSAP again consistently outperforms the HALP baseline by noticeable margins.

### 4.4. Ablations

We include ablations that demonstrate the novelty of our approach and the robustness across experiment settings.

**Adaptive perturbations.** In order to determine the importance of using adaptive weight perturbations, we can compare our method to the use of uniform perturbations throughout the entire fine-tuning process, which is equivalent to using SAM. In Table 4, we compare three different setups: Taylor pruning with SGD as a baseline, Taylor pruning with SAM, and AdaSAP<sub>P</sub>. All three settings are fine-tuned for 90 epochs. Our method outperforms both SGD and SAM at the same or smaller compressed size. This demonstrates that our method’s adaptive perturbations during the warmup phase is helping the network achieve a more prunable state.

**Robustness-aware finetuning.** In Table 4 we can also observe that enforcing robustness uniformly as in the third step

Method - % Pruned	Size ↓	Val	$R_{V2}$	$R_C$	IN-V2	IN-C
<b>SGD</b>						
Dense	1	77.32	0.84	0.54	64.79	42.46
Taylor + SGD - 80% [47]	0.20	73.56	0.82	0.46	60.56	33.93
<b>AdaSAP vs. SAM (without ASAM)</b>						
Taylor + SAM - 80% [16, 47]	0.20	73.62	0.83	0.47	61.37	34.49
<b>AdaSAP<sub>P</sub> - 80% (Ours)</b>	0.20	<b>74.38</b>	<b>0.83</b>	<b>0.48</b>	<b>62.03</b>	<b>35.86</b>
<b>AdaSAP vs. SAM (with ASAM)</b>						
SAM + ASAM - 81%	0.19	73.93	0.84	0.50	61.76	36.66
<b>AdaSAP<sub>P</sub> + ASAM - 81%</b>	0.19	<b>74.63</b>	0.83	0.50	<b>62.08</b>	<b>37.30</b>

Table 4: **Comparison of AdaSAP to SAM optimizer.** While SAM outperforms SGD, it does not match AdaSAP. This shows that adaptive weight perturbations are critical in achieving the best clean and robust performance.

Method - % Pruned	Size	Val	IN-V2	IN-C
Magnitude - 80%	0.20	$73.71 \pm 0.12$	$61.21 \pm 0.17$	$35.33 \pm 0.18$
Taylor - 80% [47]	0.20	$73.42 \pm 0.19$	$60.36 \pm 0.19$	$33.97 \pm 0.12$
EagleEye - 73% [40]	0.27	74.13	61.30	34.84
<b>AdaSAP<sub>P</sub> - 80%</b>	0.20	<b>74.54 ± 0.09</b>	<b>62.21 ± 0.13</b>	<b>37.30 ± 0.19</b>
Magnitude - 24%	0.76	$77.32 \pm 0.06$	$65.18 \pm 0.27$	$40.64 \pm 0.20$
Taylor - 24% [47]	0.76	77.05	64.53	39.68
EagleEye - 22% [40]	0.78	77.07	64.84	40.67
<b>AdaSAP<sub>P</sub> - 23%</b>	0.77	<b>78.23 ± 0.06</b>	<b>65.98 ± 0.32</b>	<b>43.43 ± 0.20</b>

Table 5: **Confidence intervals over three repeats.** Eagle-Eye checkpoints are obtained from the official repository with only one seed.

of our algorithm, regardless of ASAM or SAM, always increases both clean and robust performance above the baseline level of SGD, indicating that non-adaptive perturbations are still beneficial for generalization. See the appendix for further analysis of the choice of uniform perturbations during robustness encouragement.

**Sensitivity to importance metrics.** In our experiments, we considered  $\ell_2$  norm, or magnitude, as the saliency metric for pruning. In Table 6, we consider Taylor importance pruning [47]. As we can see, this combination still outperforms baselines in terms of robust and standard validation performance, demonstrating that our method is flexible enough to work with a variety of pruning methods.

**Confidence intervals.** We run confidence intervals on a selection of results in Table 5.

#### 4.5. Sharpness Analysis

Here we analyze the geometry of the loss landscape of the models. Consider the sharpness measure used in [16]:

$$\max_{\|\epsilon\|_2 \leq \rho} L_S(w + \epsilon) - L_S(w). \quad (9)$$

This measures the maximum amount that the loss could change if the weights are perturbed within a ball of radius  $\rho$ . We use a constant  $\rho$  to measure sharpness throughout the model. We report sharpness directly before and after pruning, to evaluate how sharpness prepares the network

Method - % Pruned	Size ↓	Val	$R_{V2}$	$R_C$	IN-V2	IN-C
Taylor + SGD - 57% [47]	0.42	75.85	0.84	0.50	63.51	37.84
AdaSAP <sub>P</sub> ,Taylor - 57% [47]	0.43	76.26	0.84	0.50	63.77	38.07
<b>AdaSAP<sub>P</sub> - 59% (Ours)</b>	<b>0.41</b>	<b>76.93</b>	<b>0.84</b>	<b>0.52</b>	<b>64.49</b>	<b>39.64</b>
Taylor + SGD - 24% [47]	0.76	77.05	0.84	0.52	64.53	39.68
AdaSAP <sub>P</sub> ,Taylor - 24% [47]	0.76	77.42	0.84	0.52	65.24	40.27
<b>AdaSAP<sub>P</sub> - 24% (Ours)</b>	<b>0.76</b>	<b>77.86</b>	<b>0.85</b>	<b>0.53</b>	<b>66.00</b>	<b>41.30</b>

Table 6: **Sensitivity to pruning criteria.** AdaSAP performs best when combined with magnitude pruning, but is flexible enough to be used with other criteria, such as Taylor importance. Here we see that AdaSAP with Taylor pruning matches or outperforms SGD with Taylor pruning. Results without ASAM.

Method - % Pruned	Size	Sharpness before pruning	Sharpness after pruning
Taylor - 58%	0.423	0.039	0.044
<b>AdaSAP<sub>P</sub> - 60% (Ours)</b>	<b>0.403</b>	<b>0.037</b>	<b>0.039</b>
Taylor - 24%	0.760	0.039	0.041
<b>AdaSAP<sub>P</sub> - 24% (Ours)</b>	<b>0.759</b>	<b>0.037</b>	<b>0.038</b>

Table 7: **Sharpness before and after pruning without finetuning.** Lower sharpness values indicates a flatter loss landscape. Results without ASAM. AdaSAP achieves flatter minima both directly before and after pruning, before any finetuning of the network.

to be optimally pruned, as well as how pruning affects the model sharpness. The results in Table 7 show that using our AdaSAP method leads to flatter models both before and after pruning. This can help explain why our models have better generalization and robust generalization performance.

## 5. Conclusion

We introduce Adaptive Sharpness-Aware Pruning (AdaSAP) which optimizes for both accuracy and robust generalization during pruning. The method consists of three steps: application of adaptive weight perturbations, pruning, and flatness-based robustness encouragement. AdaSAP outperforms a variety of SOTA pruning techniques on clean and robust performance and relative robustness in image classification and object detection.

**Limitations.** One limitation is that AdaSAP requires twice the training time due to the two backward passes necessary for optimization. Recent works [14, 43] have shown potential to cut down on this overhead. Applying these speedups to AdaSAP would be fruitful future work. Another limitation is that our analysis is based on existing robustness datasets that fall short of capturing the real world corruptions encountered in autonomous driving. Finally, despite a focus here on the more challenging structured channel pruning in this paper, we see no reason why AdaSAP would not also benefit unstructured pruning.

## References

- [1] Sajid Anwar, Kyuyeon Hwang, and Wonyong Sung. Structured pruning of deep convolutional neural networks. *ACM Journal on Emerging Technologies in Computing Systems (JETC)*, 13(3):1–18, 2017.
- [2] Aharon Azulay and Yair Weiss. Why do deep convolutional networks generalize so poorly to small image transformations? *arXiv preprint arXiv:1805.12177*, 2018.
- [3] Ron Banner, Itay Hubara, Elad Hoffer, and Daniel Soudry. Scalable methods for 8-bit training of neural networks. *Advances in neural information processing systems*, 31, 2018.
- [4] Brian Bartoldson, Ari Morcos, Adrian Barbu, and Gordon Erlebacher. The generalization-stability tradeoff in neural network pruning. *Advances in Neural Information Processing Systems*, 33:20852–20864, 2020.
- [5] Yaohui Cai, Zhewei Yao, Zhen Dong, Amir Gholami, Michael W Mahoney, and Kurt Keutzer. Zeroq: A novel zero shot quantization framework. In *Proceedings of the IEEE/CVF Conference on Computer Vision and Pattern Recognition*, pages 13169–13178, 2020.
- [6] Nicholas Carlini and David Wagner. Defensive distillation is not robust to adversarial examples. *arXiv preprint arXiv:1607.04311*, 2016.
- [7] Nicholas Carlini and David Wagner. Adversarial examples are not easily detected: Bypassing ten detection methods. In *Proceedings of the 10th ACM workshop on artificial intelligence and security*, pages 3–14, 2017.
- [8] Junbum Cha, Sanghyuk Chun, Kyungjae Lee, Han-Cheol Cho, Seunghyun Park, Yunsung Lee, and Sungrae Park. Swad: Domain generalization by seeking flat minima. *Advances in Neural Information Processing Systems*, 34:22405–22418, 2021.
- [9] Xiaoliang Dai, Peizhao Zhang, Bichen Wu, Hongxu Yin, Fei Sun, Yanghan Wang, Marat Dukhan, Yunqing Hu, Yiming Wu, Yangqing Jia, et al. Chamnet: Towards efficient network design through platform-aware model adaptation. In *Proceedings of the IEEE/CVF Conference on Computer Vision and Pattern Recognition*, pages 11398–11407, 2019.
- [10] Pau de Jorge, Amartya Sanyal, Harkirat S Behl, Philip HS Torr, Gregory Rogez, and Puneet K Dokania. Progressive skeletonization: Trimming more fat from a network at initialization. *arXiv preprint arXiv:2006.09081*, 2020.
- [11] Jia Deng, Wei Dong, Richard Socher, Li-Jia Li, Kai Li, and Li Fei-Fei. ImageNet: A large-scale hierarchical image database. In *CVPR*, 2009.
- [12] James Diffenderfer, Brian Bartoldson, Shreya Chaganti, Jize Zhang, and Bhavya Kailkhura. A winning hand: Compressing deep networks can improve out-of-distribution robustness. *Advances in Neural Information Processing Systems*, 34:664–676, 2021.
- [13] Laurent Dinh, Razvan Pascanu, Samy Bengio, and Yoshua Bengio. Sharp minima can generalize for deep nets. In *International Conference on Machine Learning*, pages 1019–1028. PMLR, 2017.
- [14] Jiawei Du, Daquan Zhou, Jiashi Feng, Vincent YF Tan, and Joey Tianyi Zhou. Sharpness-aware training for free. *arXiv preprint arXiv:2205.14083*, 2022.
- [15] M. Everingham, L. Van Gool, C. KI Williams, J. Winn, and A. Zisserman. The pascal visual object classes (voc) challenge. *IJCV*, 88:303–308, 2009.
- [16] Pierre Foret, Ariel Kleiner, Hossein Mobahi, and Behnam Neyshabur. Sharpness-aware minimization for efficiently improving generalization. *arXiv preprint arXiv:2010.01412*, 2020.
- [17] Jonathan Frankle and Michael Carbin. The lottery ticket hypothesis: Finding sparse, trainable neural networks. *arXiv preprint arXiv:1803.03635*, 2018.
- [18] Yonggan Fu, Qixuan Yu, Yang Zhang, Shang Wu, Xu Ouyang, David Cox, and Yingyan Lin. Drawing robust scratch tickets: Subnetworks with inborn robustness are found within randomly initialized networks. *Advances in Neural Information Processing Systems*, 34:13059–13072, 2021.
- [19] Amir Gholami, Sehoon Kim, Zhen Dong, Zhewei Yao, Michael W Mahoney, and Kurt Keutzer. A survey of quantization methods for efficient neural network inference. *arXiv preprint arXiv:2103.13630*, 2021.
- [20] Shuxuan Guo, Jose M Alvarez, and Mathieu Salzmann. Expandnets: Linear over-parameterization to train compact convolutional networks. *Advances in Neural Information Processing Systems*, 33:1298–1310, 2020.
- [21] Song Han, Huizi Mao, and William J Dally. Deep compression: Compressing deep neural networks with pruning, trained quantization and huffman coding. *arXiv preprint arXiv:1510.00149*, 2015.
- [22] Kaiming He, Xiangyu Zhang, Shaoqing Ren, and Jian Sun. Deep residual learning for image recognition. In *CVPR*, pages 770–778, 2016.
- [23] Yihui He, Ji Lin, Zhijian Liu, Hanrui Wang, Li-Jia Li, and Song Han. Amc: Automl for model compression and acceleration on mobile devices. In *Proceedings of the European Conference on Computer Vision (ECCV)*, pages 784–800, 2018.
- [24] Dan Hendrycks and Thomas Dietterich. Benchmarking neural network robustness to common corruptions and perturbations. *arXiv preprint arXiv:1903.12261*, 2019.
- [25] Dan Hendrycks, Mantas Mazeika, Duncan Wilson, and Kevin Gimpel. Using trusted data to train deep networks on labels corrupted by severe noise. *Advances in neural information processing systems*, 31, 2018.
- [26] Geoffrey Hinton, Oriol Vinyals, and Jeff Dean. Distilling the knowledge in a neural network. *arXiv preprint arXiv:1503.02531*, 2015.
- [27] Sepp Hochreiter and Jürgen Schmidhuber. Flat minima. *Neural computation*, 9(1):1–42, 1997.
- [28] J. Hoffmann, S. Agnihotri, T. Saikia, and T. Brox. Towards improving robustness of compressed cnns. In *ICML UDL Workshop*, 2021.
- [29] Sara Hooker, Aaron Courville, Gregory Clark, Yann Dauphin, and Andrea Frome. What do compressed deep neural networks forget? *arXiv preprint arXiv:1911.05248*, 2019.
- [30] Andrew G Howard, Menglong Zhu, Bo Chen, Dmitry Kalenichenko, Weijun Wang, Tobias Weyand, Marco An-

dreetto, and Hartwig Adam. Mobilenets: Efficient convolutional neural networks for mobile vision applications. *arXiv preprint arXiv:1704.04861*, 2017.

[31] Ryan Humble, Maying Shen, Jorge Albericio Latorre, Eric Darve, and Jose Alvarez. Soft masking for cost-constrained channel pruning. In *European Conference on Computer Vision*, pages 641–657. Springer, 2022.

[32] Yerlan Idelbayev, Pavlo Molchanov, Maying Shen, Hongxu Yin, Miguel A Carreira-Perpinán, and Jose M Alvarez. Optimal quantization using scaled codebook. In *Proceedings of the IEEE/CVF Conference on Computer Vision and Pattern Recognition*, pages 12095–12104, 2021.

[33] Pavel Izmailov, Dmitrii Podoprikhin, Timur Garipov, Dmitry Vetrov, and Andrew Gordon Wilson. Averaging weights leads to wider optima and better generalization. *arXiv preprint arXiv:1803.05407*, 2018.

[34] Yiding Jiang, Behnam Neyshabur, Hossein Mobahi, Dilip Krishnan, and Samy Bengio. Fantastic generalization measures and where to find them. *arXiv preprint arXiv:1912.02178*, 2019.

[35] Jean Kaddour, Linqing Liu, Ricardo Silva, and Matt Kusner. When do flat minima optimizers work? In *Advances in Neural Information Processing Systems*.

[36] Nitish Shirish Keskar, Dheevatsa Mudigere, Jorge Nocedal, Mikhail Smelyanskiy, and Ping Tak Peter Tang. On large-batch training for deep learning: Generalization gap and sharp minima. *arXiv preprint arXiv:1609.04836*, 2016.

[37] Jungmin Kwon, Jeongseop Kim, Hyunseo Park, and In Kwon Choi. Asam: Adaptive sharpness-aware minimization for scale-invariant learning of deep neural networks. In *International Conference on Machine Learning*, pages 5905–5914. PMLR, 2021.

[38] Y. LeCun, J. Denker, and S. Solla. Optimal brain damage. *NeurIPS*, 1989.

[39] Namhoon Lee, Thalaiyasingam Ajanthan, and Philip Torr. SNIP: Single-shot network pruning based on connection sensitivity. In *International Conference on Learning Representations*, 2019.

[40] Bailin Li, Bowen Wu, Jiang Su, and Guangrun Wang. Eageleye: Fast sub-net evaluation for efficient neural network pruning. In *European conference on computer vision*, pages 639–654. Springer, 2020.

[41] Lucas Liebenwein, Cenk Baykal, Brandon Carter, David Gifford, and Daniela Rus. Lost in pruning: The effects of pruning neural networks beyond test accuracy. *Proceedings of Machine Learning and Systems*, 3:93–138, 2021.

[42] Mingbao Lin, Rongrong Ji, Yuxin Zhang, Baochang Zhang, Yongjian Wu, and Yonghong Tian. Channel pruning via automatic structure search. *arXiv preprint arXiv:2001.08565*, 2020.

[43] Yong Liu, Siqi Mai, Xiangning Chen, Cho-Jui Hsieh, and Yang You. Towards efficient and scalable sharpness-aware minimization. In *Proceedings of the IEEE/CVF Conference on Computer Vision and Pattern Recognition*, pages 12360–12370, 2022.

[44] Zechun Liu, Haoyuan Mu, Xiangyu Zhang, Zichao Guo, Xin Yang, Kwang-Ting Cheng, and Jian Sun. Metapruning: Meta learning for automatic neural network channel pruning. In *Proceedings of the IEEE/CVF International Conference on Computer Vision*, pages 3296–3305, 2019.

[45] Aleksander Madry, Aleksandar Makelov, Ludwig Schmidt, Dimitris Tsipras, and Adrian Vladu. Towards deep learning models resistant to adversarial attacks. *arXiv preprint arXiv:1706.06083*, 2017.

[46] Pavlo Molchanov, Jimmy Hall, Hongxu Yin, Jan Kautz, Nicolo Fusi, and Arash Vahdat. Lana: latency aware network acceleration. In *European Conference on Computer Vision*, pages 137–156. Springer, 2022.

[47] Pavlo Molchanov, Arun Mallya, Stephen Tyree, Iuri Froissio, and Jan Kautz. Importance estimation for neural network pruning. In *Proceedings of the IEEE/CVF Conference on Computer Vision and Pattern Recognition*, pages 11264–11272, 2019.

[48] Pavlo Molchanov, Stephen Tyree, Tero Karras, Timo Aila, and Jan Kautz. Pruning convolutional neural networks for resource efficient inference. *arXiv preprint arXiv:1611.06440*, 2016.

[49] Clara Na, Sanket Vaibhav Mehta, and Emma Strubell. Train flat, then compress: Sharpness-aware minimization learns more compressible models. *arXiv preprint arXiv:2205.12694*, 2022.

[50] Benjamin Recht, Rebecca Roelofs, Ludwig Schmidt, and Vaishaal Shankar. Do imagenet classifiers generalize to imagenet? In *International Conference on Machine Learning*, pages 5389–5400. PMLR, 2019.

[51] Shibani Santurkar, Dimitris Tsipras, Andrew Ilyas, and Aleksander Madry. How does batch normalization help optimization? *Advances in neural information processing systems*, 31, 2018.

[52] Vikash Sehwag, Shiqi Wang, Prateek Mittal, and Suman Jana. Hydra: Pruning adversarially robust neural networks. *Advances in Neural Information Processing Systems*, 33:19655–19666, 2020.

[53] Maying Shen, Pavlo Molchanov, Hongxu Yin, and Jose M Alvarez. When to prune? a policy towards early structural pruning. In *Proceedings of the IEEE/CVF Conference on Computer Vision and Pattern Recognition*, pages 12247–12256, 2022.

[54] Maying Shen, Hongxu Yin, Pavlo Molchanov, Lei Mao, Jianna Liu, and Jose Alvarez. Structural pruning via latency-saliency knapsack. In *Advances in Neural Information Processing Systems*, 2022.

[55] Jacob Steinhardt, Pang Wei W Koh, and Percy S Liang. Certified defenses for data poisoning attacks. *Advances in neural information processing systems*, 30, 2017.

[56] David Stutz, Matthias Hein, and Bernt Schiele. Relating adversarially robust generalization to flat minima. In *Proceedings of the IEEE/CVF International Conference on Computer Vision*, pages 7807–7817, 2021.

[57] Christian Szegedy, Wojciech Zaremba, Ilya Sutskever, Joan Bruna, Dumitru Erhan, Ian Goodfellow, and Rob Fergus. Intriguing properties of neural networks. *arXiv preprint arXiv:1312.6199*, 2013.

- [58] E. Tartaglione, A. Bragagnolo, A. Fiandratti, and M. Grangetto. Loss-based sensitivity regularization: towards deep sparse neural networks. *NN*, 2022.
- [59] Chaoqi Wang, Guodong Zhang, and Roger Grosse. Picking winning tickets before training by preserving gradient flow. *arXiv preprint arXiv:2002.07376*, 2020.
- [60] Huan Wang, Can Qin, Yulun Zhang, and Yun Fu. Neural pruning via growing regularization. *arXiv preprint arXiv:2012.09243*, 2020.
- [61] Huan Wang, Can Qin, Yulun Zhang, and Yun Fu. Neural pruning via growing regularization. In *International Conference on Learning Representations*, 2021.
- [62] Dongxian Wu, Shu-Tao Xia, and Yisen Wang. Adversarial weight perturbation helps robust generalization. *Advances in Neural Information Processing Systems*, 33:2958–2969, 2020.
- [63] Lei Wu, Zhanxing Zhu, et al. Towards understanding generalization of deep learning: Perspective of loss landscapes. *arXiv preprint arXiv:1706.10239*, 2017.
- [64] Enze Xie, Wenhui Wang, Zhiding Yu, Anima Anandkumar, Jose M Alvarez, and Ping Luo. SegFormer: Simple and efficient design for semantic segmentation with transformers. In *NeurIPS*, 2021.
- [65] Huanrui Yang, Hongxu Yin, Pavlo Molchanov, Hai Li, and Jan Kautz. NViT: Vision transformer compression and parameter redistribution. *arXiv preprint arXiv:2110.04869*, 2021.
- [66] Tien-Ju Yang, Andrew Howard, Bo Chen, Xiao Zhang, Alec Go, Mark Sandler, Vivienne Sze, and Hartwig Adam. Netadapt: Platform-aware neural network adaptation for mobile applications. In *Proceedings of the European Conference on Computer Vision (ECCV)*, pages 285–300, 2018.
- [67] Hongxu Yin, Pavlo Molchanov, Jose M Alvarez, Zhizhong Li, Arun Mallya, Derek Hoiem, Niraj K Jha, and Jan Kautz. Dreaming to distill: Data-free knowledge transfer via deep-inversion. In *Proceedings of the IEEE/CVF Conference on Computer Vision and Pattern Recognition*, pages 8715–8724, 2020.
- [68] Jiahui Yu and Thomas Huang. Autoslim: Towards one-shot architecture search for channel numbers. *arXiv preprint arXiv:1903.11728*, 2019.
- [69] Jiahui Yu, Linjie Yang, Ning Xu, Jianchao Yang, and Thomas Huang. Slimmable neural networks. In *International Conference on Learning Representations*, 2019.
- [70] Shixing Yu, Zhewei Yao, Amir Gholami, Zhen Dong, Se-hoon Kim, Michael W Mahoney, and Kurt Keutzer. Hessian-aware pruning and optimal neural implant. In *Proceedings of the IEEE/CVF Winter Conference on Applications of Computer Vision*, pages 3880–3891, 2022.
- [71] Daquan Zhou, Zhiding Yu, Enze Xie, Chaowei Xiao, Animashree Anandkumar, Jiashi Feng, and Jose M Alvarez. Understanding the robustness in vision transformers. In *International Conference on Machine Learning*, pages 27378–27394. PMLR, 2022.
- [72] Tao Zhuang, Zhixuan Zhang, Yuheng Huang, Xiaoyi Zeng, Kai Shuang, and Xiang Li. Neuron-level structured pruning using polarization regularizer. *Advances in neural information processing systems*, 33:9865–9877, 2020.

## 6. Supplemental material

### 6.1. Datasets details

We conduct image classification experiments on the ImageNet dataset [11]. To evaluate the generalization ability of pruned models, we also evaluate models on ImageNet-C [24] and ImageNet-V2 [50] datasets. The former consists of the validation images from the ImageNet dataset, but with nineteen types of corruptions applied with five different levels of severity. The latter is a dataset created in the same manner as the original dataset, but consisting of different images. Therefore, it is intended to measure out of distribution performance of models. This ImageNet-V2 dataset includes three different sets, each one with a slightly different sampling strategy. We focus our experiments on the MatchedFrequencies dataset, but include evaluation all three datasets in Table 8 and see that our method consistently outperforms the baseline. Results do not use ASAM.

We conduct object detection experiments on the Pascal VOC dataset [15]. We additionally create a Pascal VOC-C dataset, in which we apply the ImageNet-C corruptions to the Pascal VOC test set. We only use one severity level.

### 6.2. Additional Robustness Datasets

As described above, we choose the ImageNet V2 Matched Frequencies dataset to perform our main set of experiments, but there are two other ImageNet V2 datasets: Threshold 0.7 and Top Images. These three datasets vary in terms of selection criteria for included images. Matched Frequencies attempts to match the image selection frequency of MTurk workers in the original ImageNet validation set. Threshold 0.7 samples from among images with a selection frequency of at least 0.7. Top Images includes the images with the highest selection frequency within each class. We provide the pruned model robustness comparison on these the additional ImageNet V2 datasets in Table 8.

Method - % Pruned	Matched Frequencies	Threshold 0.7	Top Images
Dense	64.80	73.79	79.00
Taylor - 80%	60.56	69.74	75.53
<b>AdaSAP<sub>P</sub>-80% (Ours)</b>	<b>62.03</b>	<b>70.83</b>	<b>76.62</b>
Taylor - 60%	63.51	72.54	77.83
<b>AdaSAP<sub>P</sub>-60% (Ours)</b>	<b>64.62</b>	<b>73.75</b>	<b>78.87</b>
Taylor - 24%	64.53	73.32	78.72
<b>AdaSAP<sub>P</sub>-24% (Ours)</b>	<b>66.00</b>	<b>74.70</b>	<b>79.66</b>

Table 8: Our AdaSAP method outperforms the Taylor pruning baseline on the additional ImageNet V2 datasets. Additionally, the AdaSAP model pruned to 76% outperforms the dense model across all three datasets. Results without ASAM.

### 6.3. Performance change after pruning

In Table 9 we show how the loss and accuracy change over the course of pruning. Our hypothesis is that our method sets up the network for better pruning, so that the performance drop over the course of pruning is minimized. In most cases, our method has the best validation loss and accuracy both before and after pruning. This indicates that our method sets up the model to be pruned well, and also preserves performance well throughout the pruning process.

Method - % Pruned	Val Loss Before	Val Loss After	Val Acc Before	Val Acc After
Taylor - 80%	<b>2.245</b>	3.315	<b>67.798</b>	42.915
Mag - 80%	2.416	3.288	63.843	43.21
SAM - 80%	2.255	3.2	67.577	45.802
AdaSAP <sub>P</sub> - 80% (Ours)	2.293	<b>3.146</b>	66.555	<b>46.313</b>
Taylor - 57%	2.284	2.69	66.67	57.046
Mag - 57%	2.408	2.587	63.844	59.275
SAM - 57%	2.327	2.676	65.541	57.449
AdaSAP <sub>P</sub> - 57% (Ours)	<b>2.251</b>	<b>2.574</b>	<b>67.473</b>	<b>59.962</b>
Taylor - 24%	2.441	2.42	63.389	63.711
Mag - 24%	2.292	2.406	66.714	64.087
SAM - 24%	2.401	2.379	64.019	64.589
AdaSAP <sub>P</sub> - 24% (Ours)	<b>2.213</b>	<b>2.347</b>	<b>68.463</b>	<b>65.393</b>

Table 9: Validation Loss and Accuracy directly before and after pruning (before additional fine-tuning). Across several pruning levels, our method generally reaches the lowest validation loss and accuracy both before and after pruning. Results without ASAM.

### 6.4. Varying the length of the adaptive weight perturbation step.

Throughout the main set of experiments we set to 10 the number of epochs used for the adaptive weight perturbation step. This delineates how long we use the AdaSAP optimizer for, as well as how soon into the procedure we begin pruning. In this experiment, we analyze the sensitivity of the approach to this parameter. We report results for this experiment in Table 10. We can observe that as we make this period longer, validation accuracy and ImageNet C accuracy both drop slightly, while ImageNet V2 seems to have no discernible pattern. Ratios  $R_C$  and  $R_{V2}$  also stay consistent across the experiment.

### 6.5. Robustness Encouragement

As mentioned in the main text, we consider various ablations to determine the necessity of various steps of the AdaSAP procedure. In the third step of our procedure, robustness encouragement, we choose to apply uniform perturbations across all weights in the network. This differs from the first step, in which we apply adaptive weight perturbations. In Table 11, we examine the effects of different weight perturbation strategies during the robustness encouragement phase. We can see that while all three strategies lead to relatively close final performance across the three datasets, uniform weight perturbations perform slightly bet-

Num epochs	Size ↓	Val	$R_{V2}$	$R_C$	IN-V2	IN-C
5	0.48	73.89	0.83	0.48	61.29	35.65
10	0.46	73.82	0.83	0.48	60.91	35.59
20	0.44	73.63	0.84	0.48	61.48	35.25
30	0.43	73.47	0.83	0.48	60.72	35.04

Table 10: **Effects of varying number of epochs of adaptive weight perturbation.** Increasing the number of epochs leads to smaller models but slightly worse validation and ImageNet C performance.

Perturbation Type	Val	IN-C	IN-V2
No weight perturbations	73.98	35.84	62.00
Adaptive weight perturbations	74.10	35.72	61.94
Uniform weight perturbations	<b>74.39</b>	<b>35.86</b>	<b>62.03</b>

Table 11: Comparison of various weight perturbation strategies during robustness encouragement.

Method - % Pruned	Size ↓	Val	$R_{V2}$	$R_C$	IN-V2	IN-C
<b>MobileNet-V1</b>						
Dense	1	72.63	0.82	0.45	59.30	32.79
Taylor - 60% [47]	0.40	69.61	0.80	0.42	55.90	29.51
<b>AdaSAP<sub>P</sub> - 60% (Ours)</b>	<b>0.39</b>	<b>71.05</b>	<b>0.82</b>	<b>0.44</b>	<b>58.08</b>	<b>31.06</b>
Taylor - 48% [47]	0.52	71.21	0.81	0.43	57.65	30.92
<b>AdaSAP<sub>P</sub> - 48% (Ours)</b>	<b>0.52</b>	<b>71.58</b>	<b>0.82</b>	<b>0.44</b>	<b>58.75</b>	<b>31.77</b>
EagleEye [40]	0.56	70.86	0.80	0.42	56.88	29.98
<b>AdaSAP<sub>P</sub> - 44% (Ours)</b>	<b>0.56</b>	<b>72.05</b>	<b>0.82</b>	<b>0.45</b>	<b>58.94</b>	<b>32.24</b>
<b>MobileNet-V2</b>						
Dense	1	72.10	0.81	0.45	58.50	32.40
Taylor - 28% [47]	0.72	70.49	0.81	0.43	56.87	30.22
<b>AdaSAP<sub>P</sub> - 28% (Ours)</b>	<b>0.72</b>	<b>72.06</b>	<b>0.82</b>	<b>0.45</b>	<b>58.73</b>	<b>32.63</b>
PolarReg [72]	0.87	71.72	0.82	0.45	58.46	32.04
Taylor - 12% [47]	0.88	71.93	0.82	0.45	58.75	32.21
<b>AdaSAP<sub>P</sub> - 12% (Ours)</b>	0.88	<b>72.34</b>	<b>0.82</b>	<b>0.45</b>	<b>59.28</b>	<b>32.80</b>

Table 12: **MobileNet-V1/V2 - Parameters.** Top1 Accuracy as a function of the pruning ratio.

ter, suggesting that our choice of applying them in our procedure may be slightly benefitting the performance.

## 6.6. MobileNet Results

We include results on MobileNet V1 and MobileNet V2 in Tables 12 and 13. These parallel our main results in the main paper, in which we evaluated AdaSAP<sub>P</sub> and AdaSAP<sub>L</sub> on ResNet50 and compared them against other pruning methods. Here, we perform a similar comparison, where Table 12 includes our results on AdaSAP<sub>P</sub> and Table 13 includes our results on AdaSAP<sub>L</sub>. Results here do not use ASAM. We can observe that AdaSAP performs strongly compared to baselines, particularly in the parameter-based setting.

Method - % Pruned	Speedup ↑	Val	$R_{V2}$	$R_C$	IN-V2	IN-C
<b>MobileNet-V1</b>						
Dense	1	72.63	0.82	0.45	59.30	32.79
MetaPruning [44]	2.06	66.1	—	—	—	—
AutoSlim [68]	2.27	67.9	—	—	—	—
HALP - 58% [54]	2.32	68.30	0.80	0.41	54.95	28.15
SMCP - 60% [31]	<b>2.39</b>	68.34	0.80	<b>0.42</b>	54.38	<b>28.68</b>
<b>AdaSAP<sub>L</sub> - 58% (Ours)</b>	2.33	<b>68.45</b>	<b>0.81</b>	0.41	<b>55.42</b>	28.29
0.75 MobileNetV1	1.37	68.4	—	—	—	—
AMC [23]	1.42	70.5	—	—	—	—
MetaPruning [44]	1.42	70.9	—	—	—	—
EagleEye [40]	1.47	70.86	0.80	0.42	56.88	29.98
HALP - 40% [54]	1.68	71.31	0.81	0.43	57.38	30.77
SMCP - 40% [31]	<b>1.72</b>	71.00	0.81	0.44	57.20	31.02
<b>AdaSAP<sub>L</sub> - 40% (Ours)</b>	1.70	<b>71.48</b>	<b>0.82</b>	<b>0.44</b>	<b>58.23</b>	<b>31.35</b>
<b>MobileNet-V2</b>						
Dense	1	72.10	0.81	0.45	58.50	32.40
HALP - 40% [54]	<b>1.84</b>	70.42	0.81	0.45	57.21	31.69
<b>AdaSAP<sub>L</sub> - 40% (Ours)</b>	1.81	<b>71.35</b>	0.81	<b>0.46</b>	<b>57.85</b>	<b>32.63</b>
HALP - 25% [54]	1.33	72.16	0.81	0.46	58.53	<b>33.04</b>
<b>AdaSAP<sub>L</sub> - 25% (Ours)</b>	1.39	<b>72.19</b>	<b>0.82</b>	0.46	<b>59.36</b>	32.91

Table 13: **MobileNet-V1/V2 - Latency.** Top1 accuracy for latency constrained pruning for various speedup ratios. “—” indicates that we could not evaluate the model due to unavailable code or models.

## 6.7. Full Object Detection Results

Similarly to our result on classification, we include margins of performance improvement on various corruption types for the object detection task in Figure 5.

## 6.8. Additional ablation results

In Table 14 we replicate an ablation from the main paper in which we compare AdaSAP to SAM, effectively evaluating the importance of warmup with adaptive weight perturbations. Here, we perform the comparison on a wider range of sparsities and observe that a similar pattern emerges.

## 6.9. Relative Robustness

In Figure 6 we show that AdaSAP outperforms baselines on each of the constituent elements of the relative robustness metric. Recall that relative robustness is robust accuracy divided by standard validation accuracy. In addition to outperforming baselines on relative robustness, AdaSAP also outperforms on ImageNet validation accuracy and ImageNet C robust accuracy.

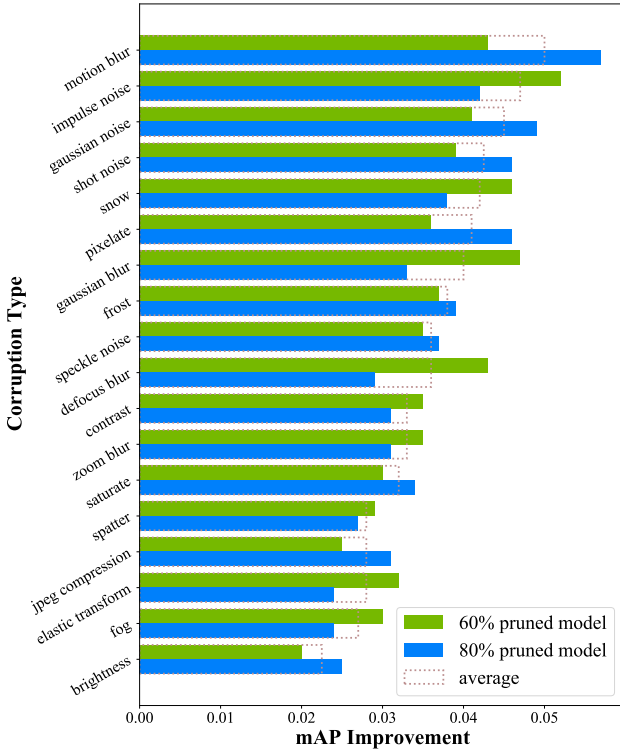


Figure 5: **Pascal VOC-C dataset.** Performance improvement per corruption as the difference between a model trained using AdaSAP minus that of a HALP pruned model.

Method - % Pruned	Size ↓	Val	$R_{V2}$	$R_C$	IN-V2	IN-C
<b>SGD</b>						
Dense	1	77.32	0.84	0.54	64.79	42.46
Taylor + SGD - 80% [47]	0.20	73.56	0.82	0.46	60.56	33.93
<b>AdaSAP vs. SAM (without ASAM)</b>						
Taylor + SAM - 80% [16, 47]	0.20	73.62	0.83	0.47	61.37	34.49
<b>AdaSAP<sub>P</sub> - 80% (Ours)</b>	0.20	<b>74.38</b>	<b>0.83</b>	<b>0.48</b>	<b>62.03</b>	<b>35.86</b>
Taylor + SGD - 58% [47]	0.42	75.85	0.84	0.50	63.51	37.84
Taylor + SAM - 57%	0.43	76.27	0.84	0.50	63.81	37.72
<b>AdaSAP<sub>P</sub> - 60% (Ours)</b>	<b>0.40</b>	<b>77.03</b>	<b>0.84</b>	<b>0.51</b>	<b>64.62</b>	<b>39.57</b>
Taylor + SGD - 24% [47]	0.76	77.05	0.84	0.52	64.53	39.68
Taylor + SAM - 24% [16, 47]	0.76	77.29	0.84	0.52	64.84	40.07
<b>AdaSAP<sub>P</sub> - 24% (Ours)</b>	0.76	<b>77.86</b>	<b>0.85</b>	<b>0.53</b>	<b>66.00</b>	<b>41.30</b>
<b>AdaSAP vs. SAM (with ASAM)</b>						
SAM + ASAM - 81%	0.19	73.93	0.84	0.50	61.76	36.66
<b>AdaSAP<sub>P</sub> + ASAM - 81%</b>	0.19	<b>74.63</b>	0.83	0.50	<b>62.08</b>	<b>37.30</b>
SAM + ASAM - 59%	0.41	77.10	0.84	0.53	64.94	40.90
<b>AdaSAP<sub>P</sub> + ASAM - 60%</b>	<b>0.40</b>	<b>77.27</b>	0.83	0.53	64.51	<b>41.23</b>

Table 14: **Comparison of AdaSAP to SAM optimizer.** AdaSAP outperforms SAM and SGD on standard validation performance and ImageNet-C performance, but slightly trails SAM on ImageNet-V2 when both methods are augmented with ASAM.

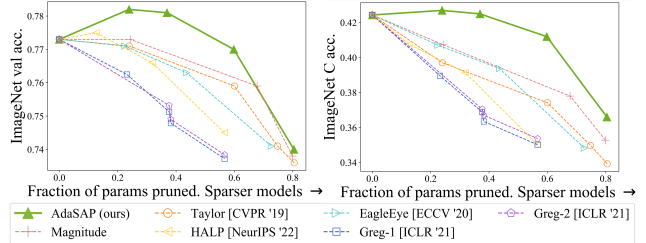


Figure 6: ImageNet Validation and ImageNet C performance on AdaSAP vs. baselines. Contains the same data as used to produce Figure 1 but demonstrates that AdaSAP additionally dominates baselines on both components of the relative robustness metric.